



## Original article



# Analytical investigation of two-dimensional fuzzy fractional heat problem using a modified approach

Jinxing Liu<sup>a</sup>, Muhammad Nadeem<sup>b</sup>, Ali Hasan Ali<sup>c,d,e,f,\*</sup>, Fawziah M. Alotaibi<sup>g</sup>  
Loredana Florentina Iambor<sup>h</sup>

<sup>a</sup> Faculty of Science, Yibin University, Yibin 644000, China

<sup>b</sup> School of Mathematics and Statistics, Qujing Normal University, Qujing 655011, China

<sup>c</sup> Department of Mathematics, College of Education for Pure Sciences, University of Basrah, 61001 Basrah, Iraq

<sup>d</sup> Institute of Mathematics, University of Debrecen, Pf. 400, H-4002 Debrecen, Hungary

<sup>e</sup> Department of Business Management, Al-inam University College, 34011 Balad, Iraq

<sup>f</sup> Jadara University Research Center, Jadara University, 21110 Irbid, Jordan

<sup>g</sup> Department of Mathematics, Turabah University College, Taif University, P.O. Box 11099, Taif 21944, Saudi Arabia

<sup>h</sup> Department of Mathematics and Computer Science, University of Oradea, 1 University Street, 410087 Oradea, Romania

## ARTICLE INFO

## Keywords:

Sumudu transform

Residual power series scheme

Fuzzy fractional heat equation

Fuzzy solution

## ABSTRACT

This paper investigates the analytical fuzzy findings of a two-dimensional fuzzy fractional-ordered heat problem including some source of terms under certain conditions. The Sumudu residual power series scheme (SRPSS) is an innovative novel to deal with the combine form of the Sumudu transform (ST) and the residual power series scheme (RPSS) which efficiently generate analytical results in rapidly converging series forms. The Caputo derivative is applied to model the physical problem. The most notable aspect of this algorithm is its ability to generate results quickly and without difficulty as compared to the conventional RPSS. We present three numerical cases of 2D heat problem with fuzzy fractional order to express the performance and validity of suggested scheme. Graphical analysis from the derived solutions reveals that SRPSS is straightforward, accurate, and suitable to analyze the findings of fuzzy fractional problems.

## 1. Introduction

Numerous researchers investigated fractional evaluation equations in recent decades because of their several applications in modern scientific and technological disciplines. It has been shown that time-fractional models explain specific physical phenomena and that their application discusses multiple challenges. In this context, it is necessary to provide more unique representations of fractional calculus [1–3]. Moreover, fractional operators offer a greater degree of freedom compared to integer differential operators in various disciplines of physical sciences and mathematical physics. Numerous researchers have used the features of operators in the context of fractional derivatives and investigated the fractional models in various fields such as; infections, bifurcates, disarray theory of control, computing images, quantum properties, fluid circulation, and a variety of relevant areas [4].

Fuzzy integral problems are useful in many real-world applications, including artificial neural networks, mathematical science, manufacturing technology, and the realm of physical sciences. Recently, It has been investigated that most of the fractional problems are transformed into unpredictable processing issues [5–7]. Fuzzy integral equations

are also important in fuzzy analytic theory and their applications in fuzzy control models, machine learning, optical science, measure concepts, and environmental science [8,9]. Consequently, numerous scholars directed their attention toward these frameworks to systematically analyze or quantify their solutions. Ali et al. [10] established the idea of Laplace transformation for the computational results of the fractional diffusion problem. Arfan et al. [11] applied an analytical technique to compute the series solution of a 2D fuzzy wave problem with some affecting component of force and presented the results in the form of a convergence series. Osman et al. [12] proposed two distinct methodologies for determining the approximate and analytical solutions of fuzzy fractional challenges. Hamoud and Ghadle [13] utilized the homotopy analysis technique to obtain the appropriate outcomes of fuzzy Volterra–Fredholm equations. The Haar wavelet approach was utilized by Ali and Hadhoud [14] to get a series of results for nonlinear fuzzy integro-differential applications. Liu et al. (2021) presented the concept of differential inclusions as a method for solving fuzzy equations. The uniqueness and various characteristics of fuzzy problems can be studied in [15–17].

\* Corresponding author.

E-mail address: [ali.hasan@science.unideb.hu](mailto:ali.hasan@science.unideb.hu) (A.H. Ali).

<https://doi.org/10.1016/j.aej.2024.07.061>

Received 5 November 2023; Received in revised form 27 June 2024; Accepted 15 July 2024

Available online 24 July 2024

1110-0168/© 2024 The Authors. Published by Elsevier B.V. on behalf of Faculty of Engineering, Alexandria University. This is an open access article under the CC BY-NC-ND license (<http://creativecommons.org/licenses/by-nc-nd/4.0/>).

Let us examine a 2D heat problem of fuzzy fractional order such as [18]:

$$D_{\vartheta}^{\alpha} \tilde{\vartheta}(\mathfrak{R}, \mathfrak{S}, \vartheta) = D_{\vartheta_1}^2 \tilde{\vartheta}(\mathfrak{R}, \mathfrak{S}, \vartheta) + D_{\vartheta_2}^2 \tilde{\vartheta}(\mathfrak{R}, \mathfrak{S}, \vartheta) + g(\mathfrak{R}, \mathfrak{S}, \vartheta), \tag{1}$$

with initial condition

$$\tilde{\vartheta}(\mathfrak{R}, \mathfrak{S}, 0) = \tilde{f}(\mathfrak{R}, \mathfrak{S}), \tag{2}$$

wherein  $\alpha$  refers to the Caputo fractional derivative. and  $g \in C([0, \infty) \times [0, \infty) \times [0, \infty), [0, \infty), [0, \infty))$ ,  $\tilde{f} \in ([0, \infty) \times [0, \infty), [0, \infty))$ . The source term indicates the presence of excessive heat production or consumption inside the system, which might result from multiple physical instances. The existence of a source term has a significant impact on the solution behaviors in the fuzzy fractional heat problem. The primary benefit of utilizing the Caputo derivative is its capacity to present the system more precisely with memory effects and long-range interactions when compared to conventional integer-order derivatives. The two-dimensional heat problem is a representation of thermal conversion that occurs in a thin sheet of infinite. The component “ $\tilde{\vartheta}$ ” in Eq. (1) reveals the climate of the body at any point in a thin sheet. The mechanism of climate transfer has the potential to be explored in a wide range of scientific and engineering problems. Consequently, there are numerous domains in which the analysis of Eq. (1) is applicable, including thermal dispersion in natural environments, thermodynamic study of intricate structures with uncertain factors, and analysis of thermal conversion in substances with unknown components.

In this research, we find a fuzzy solution to a fuzzy fractional heat problem in two dimensions by combining the Sumudu transform with the residual power series approach. The present scheme demonstrates the significant results without using any restriction on variables and assuming parameters. The clear advantage of this approach is that the resulting components of the power series lead to the exact results very swiftly. We display many visualization layouts for every case with multiple values of fractional order  $\alpha$ . The contour patterns for the lower-bound solution have a smaller quantity that represents the minimum temperature of the fuzzy heat system. In the same way, the contour patterns for the upper-bound solution have a greater quantity that represents the maximum temperature of the fuzzy heat system. In addition, we exempt the requirement of He’s polynomials which may complicate the actual problems. This study starts as follows: Section 2 includes the concept of fuzzy integrals and Sumudu transformation. We construct the scheme of SRPSS and illustrate three applications to provide the performance SRPSS in Sections 3 and 4 respectively. Finally, we provide the conclusion in Section 5.

## 2. Preliminary concept of fuzzy integral and Sumudu transform

In this part, the fundamental features and principles of the Sumudu transform are introduced, which are necessary for the construction of the SRPSS.

**Definition 2.1.** Let  $\tilde{\vartheta}$  be a continuous fuzzy component existing on the spectrum  $[0, b]$  and a subset of region  $R$ . The fuzzy fractional integral associated with  $\varphi$  can be expressed using Riemann–Liouville theory as [18]

$$\mathbf{I}^{\zeta} \tilde{\vartheta}(\varphi) = \int_0^{\varphi} \frac{(\varphi - \phi)^{\zeta-1} \tilde{\vartheta}(\phi)}{\Gamma(\zeta)} d\zeta, \phi \in (0, \infty).$$

Moreover, let  $\tilde{\vartheta} \in C^F[0, b] \cap L^F[0, b]$ , so  $C^F[0, b]$  and  $L^F[0, b]$  represents the continuity of fuzzy and its Lebesgue integrable functions. Hence, the fuzzy fractional integral is

$$\left[ \mathbf{I}^{\zeta} \tilde{\vartheta}(\varphi) \right]_{\mu} = \left[ \mathbf{I}^{\zeta} \underline{\vartheta}_{\mu}(\varphi), \mathbf{I}^{\zeta} \bar{\vartheta}_{\mu}(\varphi) \right], \quad 0 \leq \mu \leq 1,$$

hence

$$\mathbf{I}^{\zeta} \underline{\vartheta}_{\mu}(\varphi) = \int_0^{\varphi} \frac{(\varphi - \phi)^{\zeta-1} \underline{\vartheta}_{\mu}(\phi)}{\Gamma(\zeta)} d\phi, \quad \zeta, \phi \in (0, \infty),$$

$$\mathbf{I}^{\zeta} \bar{\vartheta}_{\mu}(\varphi) = \int_0^{\varphi} \frac{(\varphi - \phi)^{\zeta-1} \bar{\vartheta}_{\mu}(\phi)}{\Gamma(\zeta)} d\phi, \quad \zeta, \phi \in (0, \infty).$$

**Definition 2.2.** Assume  $\tilde{\vartheta} \in C^F[0, b] \cap L^F[0, b]$ , thus  $\left[ \underline{\vartheta}_{\mu}(\varphi), \bar{\vartheta}_{\mu}(\varphi) \right]$  where  $\mu \in [0, 1]$  and  $\varphi_0 \in (0, b)$ . Therefore, the fractional derivative in Caputo sense is stated as [18]

$$\left[ D^{\zeta} \tilde{\vartheta}(\varphi_0) \right]_{\mu} = \left[ D^{\zeta} \underline{\vartheta}_{\mu}(\varphi_0), D^{\zeta} \bar{\vartheta}_{\mu}(\varphi_0) \right], \quad 0 < \zeta \leq 1,$$

in which

$$D^{\zeta} \underline{\vartheta}_{\mu}(\varphi_0) = \left[ \int_0^{\varphi} \frac{(\varphi - \phi)^{m-\zeta-1} \frac{d^m \underline{\vartheta}_{\mu}(\phi)}{d\phi^m}}{\Gamma(m-\zeta)} d\phi \right]_{\varphi=\varphi_0},$$

$$D^{\zeta} \bar{\vartheta}_{\mu}(\varphi_0) = \left[ \int_0^{\varphi} \frac{(\varphi - \phi)^{m-\zeta-1} \frac{d^m \bar{\vartheta}_{\mu}(\phi)}{d\phi^m}}{\Gamma(m-\zeta)} d\phi \right]_{\varphi=\varphi_0}.$$

The integration term on right side can converge whereas  $m$  is rounded up to a whole number. Given that  $\zeta$  is in the range of  $(0, 1]$ , we may assume that  $m$  is equal to 1.

**Properties 1.** All fuzzy numbers containing lower and upper bounds, must meet the following constraints [19]

- (i)  $\underline{\omega}(\mu)$  be a left-continuous function with bounded and nondecreasing across the spectrum  $[0, 1]$ .
- (ii)  $\bar{\omega}(\mu)$  be a right-continuous function with bounded and nonincreasing across the spectrum  $[0, 1]$ .
- (iii)  $\underline{\omega}(\mu) \leq \bar{\omega}(\mu), \quad 0 \leq \mu \leq 1.$

Let  $\underline{\omega}(\mu) = \bar{\omega}(\mu) = \mu$ , then  $\mu$  is the crisp number.

**Definition 2.3.** The definition of the Riemann–Liouville operator for  $\alpha > 1$  is as follows [20,21]:

$$J^{\alpha} \vartheta(\vartheta) = \frac{1}{\Gamma(\alpha)} \int_0^{\vartheta} (\vartheta - \tau)^{\alpha-1} \vartheta(\tau) d\tau, \quad (\alpha > 0),$$

$$J^0 \vartheta(\vartheta) = \vartheta(\vartheta).$$

Also, we have

$$J^{\alpha} \vartheta^{\mathfrak{S}} = \frac{\Gamma(\mathfrak{S} + 1)}{\Gamma(\mathfrak{S} + \alpha + 1)} \vartheta^{\alpha + \mathfrak{S}}.$$

**Definition 2.4.** The Caputo fractional derivative is expressed as [22]:

$$D_{\vartheta}^{\alpha} \vartheta(\vartheta) = J^{\varphi-\alpha} D^{\varphi} f(\vartheta) = \frac{1}{\Gamma(n-\alpha)} \int_0^1 (\vartheta - \tau)^{\varphi-\alpha-1} \vartheta^{\varphi}(\tau) d\tau,$$

for  $\varphi - 1 < \alpha \leq \varphi, \quad \varphi \in \mathbb{N}, \quad \vartheta > 0.$

**Definition 2.5.** The ST is defined as [23]

$$A = \left\{ \vartheta(\vartheta) \mid \exists M, \tau_1, \tau_2 > 0, \mid f(\vartheta) \mid < M e^{|\vartheta|/\tau_j}, \text{ if } \vartheta \in (-1)^j \times [0, \infty) \right\},$$

thus

$$\mathbb{S}[\vartheta(\vartheta)] = \frac{1}{\vartheta} \int_0^{\infty} \vartheta(\vartheta) e^{-\frac{\vartheta}{\theta}} d\vartheta, \quad 0 < \tau_1 \leq \vartheta \leq \tau_2.$$

**Definition 2.6.** The Caputo fractional derivative of ST is explained as [24]:

$$\mathbb{S} \left[ D_{\vartheta}^{\alpha} \vartheta(\vartheta) \right] = \theta^{-\alpha} \mathbb{S}[\vartheta(\vartheta)] - \sum_{i=0}^m \theta^{-\alpha+i} \vartheta^{(i)}(0), \quad i < \alpha \leq i + 1, \quad i \in \mathbb{N}.$$

**Definition 2.7.** Let the series [25]

$$\sum_{n=0}^{\infty} \vartheta_n (\vartheta - \vartheta_0)^{n\alpha} = \vartheta_0(\mathfrak{R}) + \vartheta_1(\mathfrak{R})(\vartheta - \vartheta_0)^{\alpha} + \vartheta_2(\mathfrak{R})(\vartheta - \vartheta_0)^{2\alpha} + \dots,$$

$$0 < n - 1 < \alpha \leq n, \quad \vartheta \geq \vartheta_0.$$

be expressed as the power series about  $\vartheta = \vartheta_0$  with  $\vartheta$  as a variable and  $\mathfrak{R}$  as the coefficients of the series.

### 3. Development of SRPSS

The RPSS is a powerful approach and offers convergence series solutions to linear and nonlinear differential equations. In 2013, Arqub [26] developed the concept of RPSS by combining Taylor’s series and the residual error function for the solution of fuzzy differential equations. Later, Arqub et al. [27] studied multiple and unique procedures for RPSS to obtain quick power series solutions for nonlinear boundary value problems of time-fractional order. Many researchers showed the excellence of RPSS to various fractional PDEs such as fractional foam drainage equation [28], fractional relaxation oscillation equation [29], fractional cancer tumor models [30] and many others [31,32]

Here, we build the concept of the Sumudu residual power series scheme directly, without taking any assumptions into account. Let us assume a general 2D fuzzy fractional problem

$$D_{\theta}^{\alpha} \tilde{\delta}(\mathfrak{R}, \mathfrak{T}, \theta) = L\tilde{\delta}(\mathfrak{R}, \mathfrak{T}, \theta) + N\tilde{\delta}(\mathfrak{R}, \mathfrak{T}, \theta) + \tilde{g}(\mathfrak{R}, \mathfrak{T}, \theta), \tag{3}$$

with initial fuzzy condition

$$\tilde{\delta}(\mathfrak{R}, \mathfrak{T}, 0) = \tilde{\omega}(\mathfrak{R}, \mathfrak{T}), \tag{4}$$

**Step 1:** Applying ST on Eq. (3), it yields

$$\mathbb{S}\left[D_{\theta}^{\alpha} \tilde{\delta}(\mathfrak{R}, \mathfrak{T}, \theta)\right] = \mathbb{S}\left[L\tilde{\delta}(\mathfrak{R}, \mathfrak{T}, \theta) + N\tilde{\delta}(\mathfrak{R}, \mathfrak{T}, \theta) + \tilde{g}(\mathfrak{R}, \mathfrak{T}, \theta)\right].$$

Using the concept of ST together its fuzzy condition, we get

$$\mathbb{S}[\tilde{\delta}(\mathfrak{R}, \mathfrak{T}, \theta)] = \tilde{\omega}(\mathfrak{R}, \mathfrak{T}) + \theta^{\alpha} \left[ L\tilde{\delta}(\mathfrak{R}, \mathfrak{T}, \theta) + N\tilde{\delta}(\mathfrak{R}, \mathfrak{T}, \theta) + \tilde{g}(\mathfrak{R}, \mathfrak{T}, \theta) \right]. \tag{5}$$

**Step 2:** Taking the inverse ST on Eq. (5), we get

$$\tilde{\delta}(\mathfrak{R}, \mathfrak{T}, \theta) = \tilde{G}(\mathfrak{R}, \mathfrak{T}, \theta) + \mathbb{S}^{-1} \left[ \theta^{\alpha} \left\{ L\tilde{\delta}(\mathfrak{R}, \mathfrak{T}, \theta) + N\tilde{\delta}(\mathfrak{R}, \mathfrak{T}, \theta) \right\} \right], \tag{6}$$

where

$$\tilde{G}(\mathfrak{R}, \theta) = \tilde{\omega}(\mathfrak{R}, \mathfrak{T}) + \mathbb{S}^{-1} \left[ \theta^{\alpha} \tilde{g}(\mathfrak{R}, \mathfrak{T}, \theta) \right].$$

**Step 3:** Let us consider that Eq. (3) has the following general solution

$$\tilde{\delta}(\mathfrak{R}, \mathfrak{T}, \theta) = \sum_{n=0}^{\infty} \tilde{f}_n(\mathfrak{R}, \mathfrak{T}) \frac{\theta^{n\alpha}}{\Gamma(n\alpha + 1)}. \tag{7}$$

Then, its truncated series is

$$\tilde{\delta}_k(\mathfrak{R}, \mathfrak{T}, \theta) = \sum_{n=0}^k \tilde{f}_n(\mathfrak{R}, \mathfrak{T}) \frac{\theta^{n\alpha}}{\Gamma(n\alpha + 1)}. \tag{8}$$

**Step 4:** The concept of the residual function  $Res_{\tilde{\delta}}$  for Eq. (8) is

$$Res_{\tilde{\delta}} = \tilde{\delta}(\mathfrak{R}, \mathfrak{T}, \theta) - \left[ \tilde{G}(\mathfrak{R}, \mathfrak{T}, \theta) + \mathbb{S}^{-1} \left\{ \theta^{\alpha} \left( L\tilde{\delta}(\mathfrak{R}, \mathfrak{T}, \theta) + N\tilde{\delta}(\mathfrak{R}, \mathfrak{T}, \theta) \right) \right\} \right]. \tag{9}$$

Thus, its expression for the truncated residual function is

$$Res_{\tilde{\delta}_k} = \tilde{\delta}_k(\mathfrak{R}, \mathfrak{T}, \theta) - \left[ \tilde{G}(\mathfrak{R}, \mathfrak{T}, \theta) + \mathbb{S}^{-1} \left\{ \theta^{\alpha} \left( L\tilde{\delta}_k(\mathfrak{R}, \mathfrak{T}, \theta) + N\tilde{\delta}_k(\mathfrak{R}, \mathfrak{T}, \theta) \right) \right\} \right]. \tag{10}$$

Now, some important pinpoints of RPSS are as follows:

- $\lim_{k \rightarrow \infty} Res_{\tilde{\delta}_k}(\mathfrak{R}, \mathfrak{T}, \theta) = Res_{\tilde{\delta}}(\mathfrak{R}, \theta) = 0,$
- $D_{\theta}^{n\alpha} Res_{\tilde{\delta}_k}(\mathfrak{R}, \mathfrak{T}, 0) = 0, \quad n = 0, 1, 2, \dots$

we can obtain the subsequent outcomes:

$$\tilde{\delta}_n(\mathfrak{R}, \mathfrak{T}, \theta) = \tilde{\delta}_0(\mathfrak{R}, \mathfrak{T}, \theta) + \tilde{\delta}_1(\mathfrak{R}, \mathfrak{T}, \theta) + \tilde{\delta}_2(\mathfrak{R}, \mathfrak{T}, \theta) + \tilde{\delta}_3(\mathfrak{R}, \mathfrak{T}, \theta) + \dots,$$

such that

$$\tilde{\delta}(\mathfrak{R}, \mathfrak{T}, \theta) = \lim_{N \rightarrow \infty} \sum_{n=0}^N \tilde{\delta}_n(\mathfrak{R}, \mathfrak{T}, \theta),$$

where

$$\tilde{\delta}_0(\mathfrak{R}, \mathfrak{T}, \theta) = \tilde{\delta}(\mathfrak{R}, \mathfrak{T}, 0),$$

$$\tilde{\delta}_1(\mathfrak{R}, \mathfrak{T}, \theta) = \tilde{f}_1(\mathfrak{R}, \mathfrak{T}) \frac{\theta^{\alpha}}{\Gamma(1 + \alpha)},$$

$$\tilde{\delta}_2(\mathfrak{R}, \mathfrak{T}, \theta) = \tilde{f}_2(\mathfrak{R}, \mathfrak{T}) \frac{\theta^{2\alpha}}{\Gamma(1 + 2\alpha)},$$

⋮

$$\tilde{\delta}_n(\mathfrak{R}, \mathfrak{T}, \theta) = \tilde{f}_n(\mathfrak{R}, \mathfrak{T}) \frac{\theta^{n\alpha}}{\Gamma(1 + n\alpha)}.$$

Therefore, the estimated outcomes obtained from SRPSS are as follows:

$$\tilde{\delta}(\mathfrak{R}, \mathfrak{T}, \theta) = \tilde{\delta}_0(\mathfrak{R}, \mathfrak{T}, \theta) + \tilde{\delta}_1(\mathfrak{R}, \mathfrak{T}, \theta) + \tilde{\delta}_2(\mathfrak{R}, \mathfrak{T}, \theta) + \tilde{\delta}_3(\mathfrak{R}, \mathfrak{T}, \theta) + \dots$$

### 4. Numerical applications

This section showcases the effectiveness of SRPSS in acquiring the fuzzy outcomes of a 2D heat problem of fuzzy fractional order  $\alpha$ . In this analysis, we examine three specific examples and calculate the solutions for both the lower and upper bounds at various fractional orders. The upper-bound and lower-bound results are derived by considering the maximum and minimum range of uncertain parameters in this model. The findings are displayed as a fractional series of power that converge to the precise outcomes. These outcomes are computed using the Mathematica programming.

#### 4.1. Example 1

Let us examine the two-dimensional time-fractional fuzzy heat problem

$$D_{\theta}^{\alpha} \tilde{\delta}(\mathfrak{R}, \mathfrak{T}, \theta) = \tilde{\delta}_{\mathfrak{R}\mathfrak{R}}(\mathfrak{R}, \mathfrak{T}, \theta) + \tilde{\delta}_{\mathfrak{T}\mathfrak{T}}(\mathfrak{R}, \mathfrak{T}, \theta) + \mathfrak{R} + \mathfrak{T} + \theta, \tag{11}$$

subject to

$$\tilde{\delta}(\mathfrak{R}, \mathfrak{T}, 0) = \tilde{\omega}e^{-(\mathfrak{R}+\mathfrak{T})}. \tag{12}$$

here  $\tilde{\omega} = [\underline{\omega}, \bar{\omega}] = [\mu - 1, 1 - \mu].$

##### 4.1.1. Lower bound findings for $\tilde{\delta}(\mathfrak{R}, \mathfrak{T}, \theta)$

From Eq. (11), we can write the lower bound fuzzy problem as follows

$$\frac{\partial^{\alpha} g}{\partial \theta^{\alpha}} = \frac{\partial^2 g}{\partial \mathfrak{R}^2} + \frac{\partial^2 g}{\partial \mathfrak{T}^2} + \mathfrak{R} + \mathfrak{T} + \theta, \tag{13}$$

with the initial condition

$$g(\mathfrak{R}, \mathfrak{T}, 0) = (\mu - 1)e^{-(\mathfrak{R}+\mathfrak{T})}. \tag{14}$$

Taking ST, we get

$$\mathbb{S}\left[\frac{\partial^{\alpha} g}{\partial \theta^{\alpha}}\right] = \mathbb{S}\left[\frac{\partial^2 g}{\partial \mathfrak{R}^2} + \frac{\partial^2 g}{\partial \mathfrak{T}^2} + \mathfrak{R} + \mathfrak{T} + \theta\right].$$

Employing the definition of ST under the Caputo fractional operator, it gives

$$\mathbb{S}[g(\mathfrak{R}, \mathfrak{T}, \theta)] = (\mu - 1)e^{-(\mathfrak{R}+\mathfrak{T})} + \theta^{\alpha} \mathbb{S}\left[\frac{\partial^2 g}{\partial \mathfrak{R}^2} + \frac{\partial^2 g}{\partial \mathfrak{T}^2} + \mathfrak{R} + \mathfrak{T} + \theta\right].$$

Applying inverse ST, we obtain

$$g(\mathfrak{R}, \mathfrak{T}, \theta) = (\mu - 1)e^{-(\mathfrak{R}+\mathfrak{T})} + \mathbb{S}^{-1} \left[ \theta^{\alpha} \left\{ S\left(\frac{\partial^2 g}{\partial \mathfrak{R}^2} + \frac{\partial^2 g}{\partial \mathfrak{T}^2} + \mathfrak{R} + \mathfrak{T} + \theta\right) \right\} \right].$$

Using the aforementioned approach, we receive the iterations as follows:

$$\underline{\delta}_1(\zeta, \mu, \tau) = 2(\mu - 1)e^{-(\mathfrak{R}+\mathfrak{T})} \frac{\theta^{\alpha}}{\Gamma(\alpha + 1)},$$

$$\underline{\delta}_2(\mathfrak{R}, \mathfrak{T}, \theta) = 4(\mu - 1)e^{-(\mathfrak{R}+\mathfrak{T})} \frac{\theta^{2\alpha}}{\Gamma(2\alpha + 1)},$$

$$\underline{\delta}_3(\mathfrak{R}, \mathfrak{T}, \theta) = 8(\mu - 1)e^{-(\mathfrak{R}+\mathfrak{T})} \frac{\theta^{3\alpha}}{\Gamma(3\alpha + 1)},$$

⋮

Consequently, these results can be written as follows:

$$\begin{aligned} \underline{\vartheta}(\mathfrak{R}, \mathfrak{S}, \vartheta) &= \underline{\vartheta}_0(\mathfrak{R}, \mathfrak{S}, \vartheta) + \underline{\vartheta}_1(\mathfrak{R}, \mathfrak{S}, \vartheta) + \underline{\vartheta}_2(\mathfrak{R}, \mathfrak{S}, \vartheta) + \underline{\vartheta}_3(\mathfrak{R}, \mathfrak{S}, \vartheta) + \dots, \\ &= (\mu - 1)e^{-(\mathfrak{R}+\mathfrak{S})} + \mathfrak{R} \frac{\vartheta^\alpha}{\Gamma(\alpha+1)} + \mathfrak{S} \frac{\vartheta^\alpha}{\Gamma(\alpha+1)} + \frac{\vartheta^{\alpha+1}}{\Gamma(\alpha+2)} \\ &+ 2(\mu - 1)e^{-(\mathfrak{R}+\mathfrak{S})} \frac{\vartheta^\alpha}{\Gamma(\alpha+1)} \\ &+ 4(\mu - 1)e^{-(\mathfrak{R}+\mathfrak{S})} \frac{\vartheta^{2\alpha}}{\Gamma(2\alpha+1)} + 8(\mu - 1)e^{-(\mathfrak{R}+\mathfrak{S})} \frac{\vartheta^{3\alpha}}{\Gamma(3\alpha+1)} + \dots \end{aligned} \tag{15}$$

**Remark.** If  $g(\mathfrak{R}, \mathfrak{S}, \vartheta) = 0$ , then above equation becomes as

$$\begin{aligned} \underline{\vartheta}(\mathfrak{R}, \mathfrak{S}, \vartheta) &= (\mu - 1)e^{-(\mathfrak{R}+\mathfrak{S})} + 2(\mu - 1)e^{-(\mathfrak{R}+\mathfrak{S})} \frac{\vartheta^\alpha}{\Gamma(\alpha+1)} \\ &+ 4(\mu - 1)e^{-(\mathfrak{R}+\mathfrak{S})} \frac{\vartheta^{2\alpha}}{\Gamma(2\alpha+1)} + 8(\mu - 1)e^{-(\mathfrak{R}+\mathfrak{S})} \frac{\vartheta^{3\alpha}}{\Gamma(3\alpha+1)} + \dots, \\ &= (\mu - 1)e^{-(\mathfrak{R}+\mathfrak{S})} \left[ 1 + 2 \frac{\vartheta^\alpha}{\Gamma(\alpha+1)} + 4 \frac{\vartheta^{2\alpha}}{\Gamma(2\alpha+1)} \right. \\ &\left. + 8 \frac{\vartheta^{3\alpha}}{\Gamma(3\alpha+1)} + \dots \right]. \end{aligned} \tag{16}$$

It can be in closed form

$$\underline{\vartheta}(\mathfrak{R}, \mathfrak{S}, \vartheta) = (\mu - 1)e^{-(\mathfrak{R}+\mathfrak{S})} \sum_{n=0}^{\infty} \frac{(2\vartheta^\alpha)^n}{\Gamma(n\alpha+1)}. \tag{17}$$

#### 4.1.2. Upper bound findings for $\bar{\vartheta}(\mathfrak{R}, \mathfrak{S}, \vartheta)$

From Eq. (11), we can write the upper bound fuzzy problem as follows

$$\frac{\partial^\alpha \bar{\vartheta}}{\partial \vartheta^\alpha} = \frac{\partial^2 \bar{\vartheta}}{\partial \mathfrak{R}^2} + \frac{\partial^2 \bar{\vartheta}}{\partial \mathfrak{S}^2} + \mathfrak{R} + \mathfrak{S} + \vartheta, \tag{18}$$

with the initial condition

$$\bar{\vartheta}(\mathfrak{R}, \mathfrak{S}, 0) = (1 - \mu)e^{-(\mathfrak{R}+\mathfrak{S})}. \tag{19}$$

Using the aforementioned approach, we receive the subsequent outcomes:

$$\begin{aligned} \bar{\vartheta}_0(\mathfrak{R}, \mathfrak{S}, \vartheta) &= (1 - \mu)e^{-(\mathfrak{R}+\mathfrak{S})} + \mathfrak{R} \frac{\vartheta^\alpha}{\Gamma(\alpha+1)} + \mathfrak{S} \frac{\vartheta^\alpha}{\Gamma(\alpha+1)} + \frac{\vartheta^{\alpha+1}}{\Gamma(\alpha+2)}, \\ \bar{\vartheta}_1(\mathfrak{R}, \mathfrak{S}, \vartheta) &= 2(1 - \mu)e^{-(\mathfrak{R}+\mathfrak{S})} \frac{\vartheta^\alpha}{\Gamma(\alpha+1)}, \\ \bar{\vartheta}_2(\mathfrak{R}, \mathfrak{S}, \vartheta) &= 4(1 - \mu)e^{-(\mathfrak{R}+\mathfrak{S})} \frac{\vartheta^{2\alpha}}{\Gamma(2\alpha+1)}, \\ \bar{\vartheta}_3(\mathfrak{R}, \mathfrak{S}, \vartheta) &= 8(1 - \mu)e^{-(\mathfrak{R}+\mathfrak{S})} \frac{\vartheta^{3\alpha}}{\Gamma(3\alpha+1)}, \\ &\vdots \end{aligned}$$

Consequently, these results can be written as follows:

$$\begin{aligned} \bar{\vartheta}(\mathfrak{R}, \mathfrak{S}, \vartheta) &= \bar{\vartheta}_0(\mathfrak{R}, \mathfrak{S}, \vartheta) + \bar{\vartheta}_1(\mathfrak{R}, \mathfrak{S}, \vartheta) + \bar{\vartheta}_2(\mathfrak{R}, \mathfrak{S}, \vartheta) + \bar{\vartheta}_3(\mathfrak{R}, \mathfrak{S}, \vartheta) + \dots, \\ &= (1 - \mu)e^{-(\mathfrak{R}+\mathfrak{S})} + \mathfrak{R} \frac{\vartheta^\alpha}{\Gamma(\alpha+1)} + \mathfrak{S} \frac{\vartheta^\alpha}{\Gamma(\alpha+1)} + \frac{\vartheta^{\alpha+1}}{\Gamma(\alpha+2)} \\ &+ 2(1 - \mu)e^{-(\mathfrak{R}+\mathfrak{S})} \frac{\vartheta^\alpha}{\Gamma(\alpha+1)} \\ &+ 4(1 - \mu)e^{-(\mathfrak{R}+\mathfrak{S})} \frac{\vartheta^{2\alpha}}{\Gamma(2\alpha+1)} + 8(1 - \mu)e^{-(\mathfrak{R}+\mathfrak{S})} \frac{\vartheta^{3\alpha}}{\Gamma(3\alpha+1)} + \dots \end{aligned} \tag{20}$$

**Remark.** If  $g(\mathfrak{R}, \mathfrak{S}, \vartheta) = 0$ , then above equation becomes as

$$\begin{aligned} \bar{\vartheta}(\mathfrak{R}, \mathfrak{S}, \vartheta) &= (1 - \mu)e^{-(\mathfrak{R}+\mathfrak{S})} + 2(1 - \mu)e^{-(\mathfrak{R}+\mathfrak{S})} \frac{\vartheta^\alpha}{\Gamma(\alpha+1)} \\ &+ 4(1 - \mu)e^{-(\mathfrak{R}+\mathfrak{S})} \frac{\vartheta^{2\alpha}}{\Gamma(2\alpha+1)} + 8(1 - \mu)e^{-(\mathfrak{R}+\mathfrak{S})} \frac{\vartheta^{3\alpha}}{\Gamma(3\alpha+1)} + \dots, \end{aligned}$$

$$\begin{aligned} &= (1 - \mu)e^{-(\mathfrak{R}+\mathfrak{S})} \left[ 1 + 2 \frac{\vartheta^\alpha}{\Gamma(\alpha+1)} + 4 \frac{\vartheta^{2\alpha}}{\Gamma(2\alpha+1)} \right. \\ &\left. + 8 \frac{\vartheta^{3\alpha}}{\Gamma(3\alpha+1)} + \dots \right]. \end{aligned} \tag{21}$$

It can be in closed form

$$\bar{\vartheta}(\mathfrak{R}, \mathfrak{S}, \vartheta) = (1 - \mu)e^{-(\mathfrak{R}+\mathfrak{S})} \sum_{n=0}^{\infty} \frac{(2\vartheta^\alpha)^n}{\Gamma(n\alpha+1)}. \tag{22}$$

Fig. 1 is divided into four parts, showcasing the lower bound fuzzy findings for various fractional orders of  $\alpha$ . Figs. 1(a) and 1(c) present the lower bound surfaces results with space components  $\mu = 0.4$ ,  $0 \leq \mathfrak{R} \leq 5$ ,  $0 \leq \mathfrak{S} \leq 5$  upon  $\alpha = 0.5$  and  $\alpha = 1$  respectively. Similarly, Figs. 1(b) and 1(d) reveal the lower bound contour results with space components  $\mu = 0.4$ ,  $-1 \leq \mathfrak{R} \leq 1$ ,  $-1 \leq \mathfrak{S} \leq 1$  upon  $\alpha = 0.5$  and  $\alpha = 1$  respectively. Fig. 2 is divided into four parts, showcasing the upper bound fuzzy findings for various fractional orders of  $\alpha$ . Figs. 2(a) and 2(c) present the upper bound surfaces results with space components  $\mu = 0.4$ ,  $0 \leq \mathfrak{R} \leq 1$ ,  $0 \leq \mathfrak{S} \leq 1$  upon  $\alpha = 0.5$  and  $\alpha = 1$  respectively. Similarly, Figs. 2(b) and 2(d) reveal the upper bound contour results with space components  $\mu = 0.4$ ,  $-1 \leq \mathfrak{R} \leq 1$ ,  $-1 \leq \mathfrak{S} \leq 1$  upon  $\alpha = 0.5$  and  $\alpha = 1$  respectively. We consider the amount of  $\vartheta = 0.1$  for lower and upper bound surface and contour fuzzy results respectively, On observing, the fractional order on both values gives excellent results to show that our proposed approach is legitimate and robust for the fuzzy fractional problems. Fig. 3 states the 2D fuzzy plot for lower and upper bound results when  $\mu = 0.4$  and  $\mu = 0.8$ .

#### 4.2. Example 2

Let us examine another two-dimensional time-fractional fuzzy heat problem

$$D_\vartheta^\alpha \bar{\vartheta}(\mathfrak{R}, \mathfrak{S}, \vartheta) = \bar{\vartheta}_{\mathfrak{R}\mathfrak{R}}(\mathfrak{R}, \mathfrak{S}, \vartheta) + \bar{\vartheta}_{\mathfrak{S}\mathfrak{S}}(\mathfrak{R}, \mathfrak{S}, \vartheta) + \mathfrak{R} + \mathfrak{S} + \vartheta^2, \tag{23}$$

with the initial condition

$$\bar{\vartheta}(\mathfrak{R}, \mathfrak{S}, 0) = \bar{\omega} \sin[\pi(\mathfrak{R} + \mathfrak{S})]. \tag{24}$$

here  $\bar{\omega} = [\underline{\omega}, \bar{\omega}] = [\mu - 1, 1 - \mu]$ .

##### 4.2.1. Lower bound findings for $\bar{\vartheta}(\mathfrak{R}, \mathfrak{S}, \vartheta)$

From Eq. (23), we can write the lower bound fuzzy problem as follows

$$\frac{\partial^\alpha \bar{\vartheta}}{\partial \vartheta^\alpha} = \frac{\partial^2 \bar{\vartheta}}{\partial \mathfrak{R}^2} + \frac{\partial^2 \bar{\vartheta}}{\partial \mathfrak{S}^2} + \mathfrak{R} + \mathfrak{S} + \vartheta^2, \tag{25}$$

with the initial condition

$$\underline{\vartheta}(\mathfrak{R}, \mathfrak{S}, 0) = (\mu - 1) \sin[\pi(\mathfrak{R} + \mathfrak{S})]. \tag{26}$$

Using the aforementioned approach, we receive the subsequent outcomes:

$$\begin{aligned} \underline{\vartheta}_0(\mathfrak{R}, \mathfrak{S}, \vartheta) &= (\mu - 1) \sin[\pi(\mathfrak{R} + \mathfrak{S})] + \mathfrak{R} \frac{\vartheta^\alpha}{\Gamma(\alpha+1)} + \mathfrak{S} \frac{\vartheta^\alpha}{\Gamma(\alpha+1)} \\ &+ 2 \frac{\vartheta^{\alpha+2}}{\Gamma(\alpha+2)}, \\ \underline{\vartheta}_1(\mathfrak{R}, \mathfrak{S}, \vartheta) &= -2(\mu - 1)\pi^2 \sin[\pi(\mathfrak{R} + \mathfrak{S})] \frac{\vartheta^\alpha}{\Gamma(\alpha+1)}, \\ \underline{\vartheta}_2(\mathfrak{R}, \mathfrak{S}, \vartheta) &= 4(\mu - 1)\pi^2 \sin[\pi(\mathfrak{R} + \mathfrak{S})] \frac{\vartheta^{2\alpha}}{\Gamma(2\alpha+1)}, \\ \underline{\vartheta}_3(\mathfrak{R}, \mathfrak{S}, \vartheta) &= -8(\mu - 1)\pi^2 \sin[\pi(\mathfrak{R} + \mathfrak{S})] \frac{\vartheta^{3\alpha}}{\Gamma(3\alpha+1)}, \\ &\vdots \end{aligned}$$

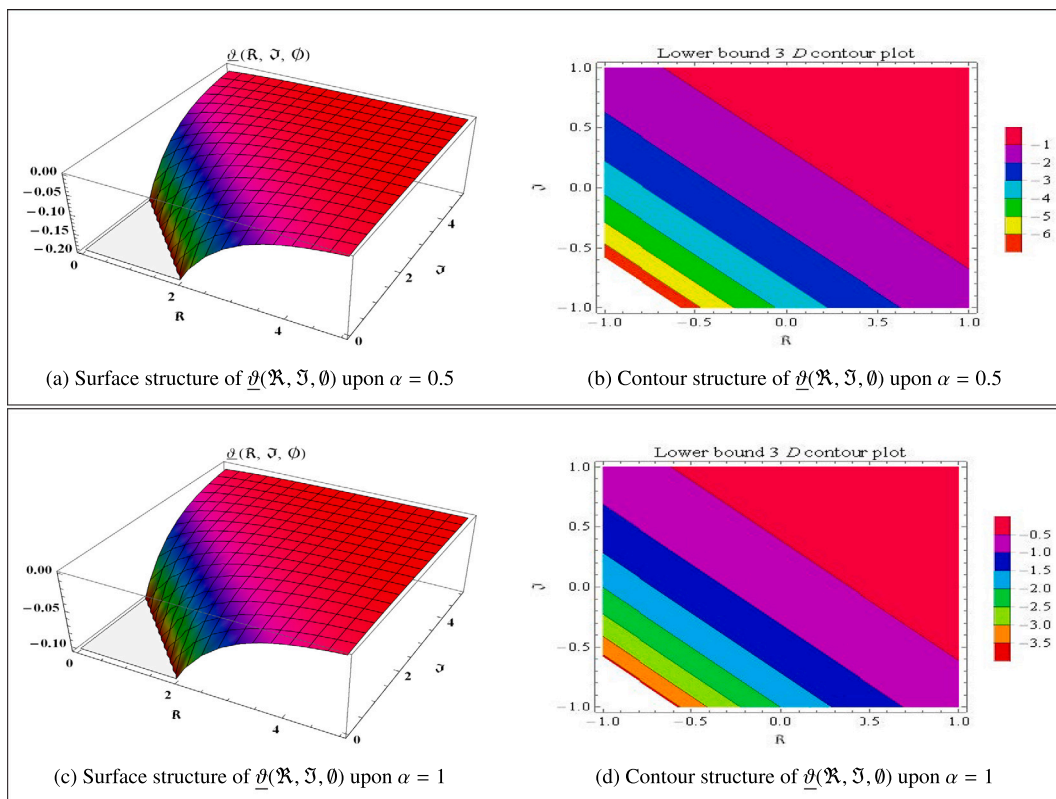


Fig. 1. 3D surface and contour plots of  $\underline{\vartheta}(\mathfrak{R}, \mathfrak{J}, \theta)$  solutions with  $\alpha = 0.5, 1$  for Example (4.1).

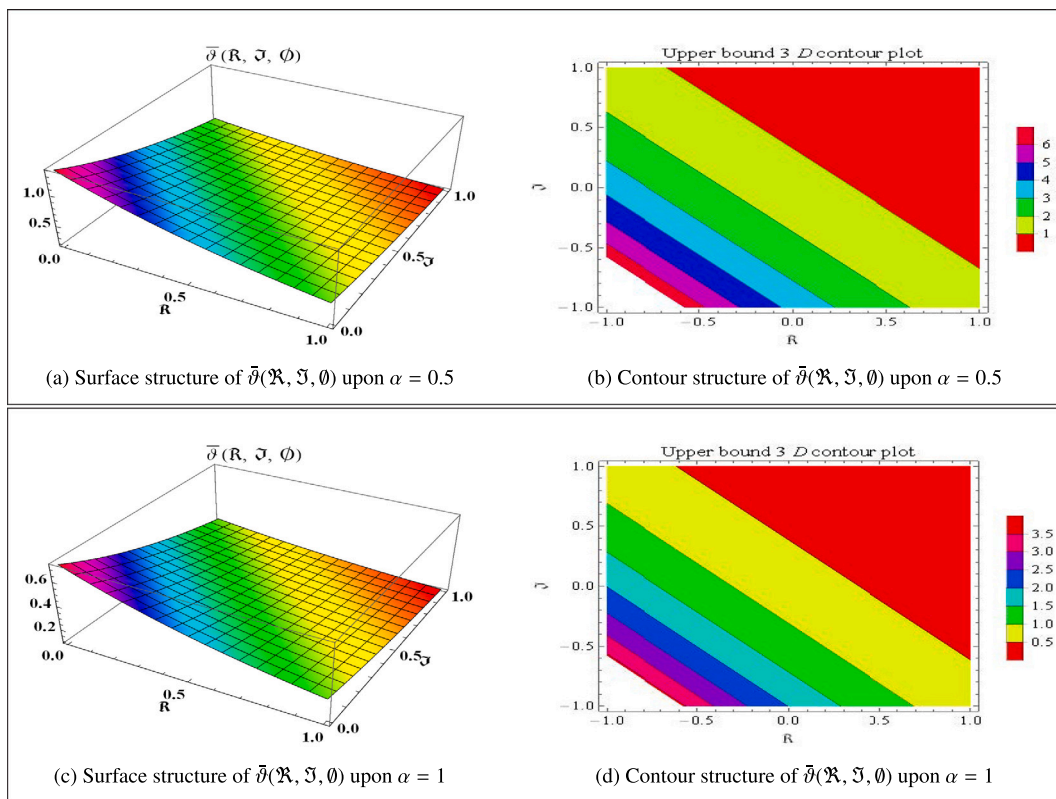


Fig. 2. 3D surface and contour plots of  $\bar{\vartheta}(\mathfrak{R}, \mathfrak{J}, \theta)$  solutions with  $\alpha = 0.5, 1$  for Example (4.1).

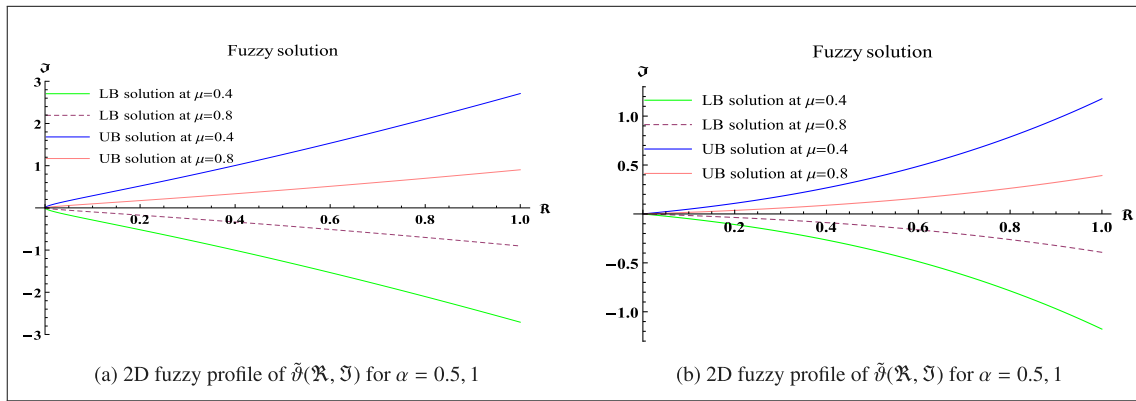


Fig. 3. 2D fuzzy  $\tilde{\vartheta}(\mathfrak{R}, \mathfrak{S})$  solutions on different fractional order for Example (4.1).

Consequently, these results can be written as follows:

$$\begin{aligned} \underline{\vartheta}(\mathfrak{R}, \mathfrak{S}, \vartheta) &= \underline{\vartheta}_0(\mathfrak{R}, \mathfrak{S}, \vartheta) + \underline{\vartheta}_1(\mathfrak{R}, \mathfrak{S}, \vartheta) + \underline{\vartheta}_2(\mathfrak{R}, \mathfrak{S}, \vartheta) + \underline{\vartheta}_3(\mathfrak{R}, \mathfrak{S}, \vartheta) + \dots, \\ &= (\mu - 1) \sin[\pi(\mathfrak{R} + \mathfrak{S})] + \mathfrak{R} \frac{\vartheta^\alpha}{\Gamma(\alpha + 1)} + \mathfrak{S} \frac{\vartheta^\alpha}{\Gamma(\alpha + 1)} \\ &+ 2 \frac{\vartheta^{\alpha+2}}{\Gamma(\alpha + 2)} - 2(\mu - 1)\pi^2 \sin[\pi(\mathfrak{R} + \mathfrak{S})] \frac{\vartheta^\alpha}{\Gamma(\alpha + 1)} \\ &+ 4(\mu - 1)\pi^2 \sin[\pi(\mathfrak{R} + \mathfrak{S})] \frac{\vartheta^{2\alpha}}{\Gamma(2\alpha + 1)} \\ &- 8(\mu - 1)\pi^2 \sin[\pi(\mathfrak{R} + \mathfrak{S})] \frac{\vartheta^{3\alpha}}{\Gamma(3\alpha + 1)} + \dots. \end{aligned} \tag{27}$$

**Remark.** If  $g(\mathfrak{R}, \mathfrak{S}, \vartheta) = 0$ , then above equation becomes as

$$\begin{aligned} \underline{\vartheta}(\mathfrak{R}, \mathfrak{S}, \vartheta) &= (\mu - 1) \sin[\pi(\mathfrak{R} + \mathfrak{S})] - 2(\mu - 1)\pi^2 \sin[\pi(\mathfrak{R} + \mathfrak{S})] \frac{\vartheta^\alpha}{\Gamma(\alpha + 1)} \\ &+ 4(\mu - 1)\pi^2 \sin[\pi(\mathfrak{R} + \mathfrak{S})] \frac{\vartheta^{2\alpha}}{\Gamma(2\alpha + 1)} \\ &- 8(\mu - 1)\pi^2 \sin[\pi(\mathfrak{R} + \mathfrak{S})] \frac{\vartheta^{3\alpha}}{\Gamma(3\alpha + 1)} + \dots. \end{aligned} \tag{28}$$

It can be in closed form

$$\underline{\vartheta}(\mathfrak{R}, \mathfrak{S}, \vartheta) = (\mu - 1) \sin[\pi(\mathfrak{R} + \mathfrak{S})] \sum_{n=0}^{\infty} \frac{(-1)^n (2\pi^2 \vartheta^\alpha)^n}{\Gamma(n\alpha + 1)}. \tag{29}$$

4.2.2. Upper bound findings for  $\tilde{\vartheta}(\mathfrak{R}, \mathfrak{S}, \vartheta)$

From Eq. (23), we can write the lower bound fuzzy problem as follows

$$\frac{\partial^\alpha \tilde{\vartheta}}{\partial \vartheta^\alpha} = \frac{\partial^2 \tilde{\vartheta}}{\partial \mathfrak{R}^2} + \frac{\partial^2 \tilde{\vartheta}}{\partial \mathfrak{S}^2} + \mathfrak{R} + \mathfrak{S} + \vartheta^2, \tag{30}$$

with the initial condition

$$\tilde{\vartheta}(\mathfrak{R}, \mathfrak{S}, 0) = (1 - \mu) \sin[\pi(\mathfrak{R} + \mathfrak{S})]. \tag{31}$$

Using the aforementioned approach, we receive the subsequent outcomes:

$$\begin{aligned} \bar{\vartheta}_0(\mathfrak{R}, \mathfrak{S}, \vartheta) &= (1 - \mu) \sin[\pi(\mathfrak{R} + \mathfrak{S})] + \mathfrak{R} \frac{\vartheta^\alpha}{\Gamma(\alpha + 1)} + \mathfrak{S} \frac{\vartheta^\alpha}{\Gamma(\alpha + 1)} \\ &+ 2 \frac{\vartheta^{\alpha+2}}{\Gamma(\alpha + 2)}, \\ \bar{\vartheta}_1(\mathfrak{R}, \mathfrak{S}, \vartheta) &= -2(1 - \mu)\pi^2 \sin[\pi(\mathfrak{R} + \mathfrak{S})] \frac{\vartheta^\alpha}{\Gamma(\alpha + 1)}, \\ \bar{\vartheta}_2(\mathfrak{R}, \mathfrak{S}, \vartheta) &= 4(1 - \mu)\pi^2 \sin[\pi(\mathfrak{R} + \mathfrak{S})] \frac{\vartheta^{2\alpha}}{\Gamma(2\alpha + 1)}, \\ \bar{\vartheta}_3(\mathfrak{R}, \mathfrak{S}, \vartheta) &= -8(1 - \mu)\pi^2 \sin[\pi(\mathfrak{R} + \mathfrak{S})] \frac{\vartheta^{3\alpha}}{\Gamma(3\alpha + 1)}, \end{aligned}$$

∴

Consequently, these results can be written as follows:

$$\begin{aligned} \bar{\vartheta}(\mathfrak{R}, \mathfrak{S}, \vartheta) &= \bar{\vartheta}_0(\mathfrak{R}, \mathfrak{S}, \vartheta) + \bar{\vartheta}_1(\mathfrak{R}, \mathfrak{S}, \vartheta) + \bar{\vartheta}_2(\mathfrak{R}, \mathfrak{S}, \vartheta) + \bar{\vartheta}_3(\mathfrak{R}, \mathfrak{S}, \vartheta) + \dots, \\ &= (1 - \mu) \sin[\pi(\mathfrak{R} + \mathfrak{S})] + \mathfrak{R} \frac{\vartheta^\alpha}{\Gamma(\alpha + 1)} + \mathfrak{S} \frac{\vartheta^\alpha}{\Gamma(\alpha + 1)} \\ &+ 2 \frac{\vartheta^{\alpha+2}}{\Gamma(\alpha + 2)} - 2(1 - \mu)\pi^2 \sin[\pi(\mathfrak{R} + \mathfrak{S})] \frac{\vartheta^\alpha}{\Gamma(\alpha + 1)} \\ &+ 4(1 - \mu)\pi^2 \sin[\pi(\mathfrak{R} + \mathfrak{S})] \frac{\vartheta^{2\alpha}}{\Gamma(2\alpha + 1)} \\ &- 8(1 - \mu)\pi^2 \sin[\pi(\mathfrak{R} + \mathfrak{S})] \frac{\vartheta^{3\alpha}}{\Gamma(3\alpha + 1)} + \dots. \end{aligned} \tag{32}$$

**Remark.** If  $g(\mathfrak{R}, \mathfrak{S}, \vartheta) = 0$ , then above equation becomes as

$$\begin{aligned} \bar{\vartheta}(\mathfrak{R}, \mathfrak{S}, \vartheta) &= (1 - \mu) \sin[\pi(\mathfrak{R} + \mathfrak{S})] - 2(1 - \mu)\pi^2 \sin[\pi(\mathfrak{R} + \mathfrak{S})] \frac{\vartheta^\alpha}{\Gamma(\alpha + 1)} \\ &+ 4(1 - \mu)\pi^2 \sin[\pi(\mathfrak{R} + \mathfrak{S})] \frac{\vartheta^{2\alpha}}{\Gamma(2\alpha + 1)} \\ &- 8(1 - \mu)\pi^2 \sin[\pi(\mathfrak{R} + \mathfrak{S})] \frac{\vartheta^{3\alpha}}{\Gamma(3\alpha + 1)} + \dots. \end{aligned} \tag{33}$$

It can be in closed form

$$\bar{\vartheta}(\mathfrak{R}, \mathfrak{S}, \vartheta) = (1 - \mu) \sin[\pi(\mathfrak{R} + \mathfrak{S})] \sum_{n=0}^{\infty} \frac{(-1)^n (2\pi^2 \vartheta^\alpha)^n}{\Gamma(n\alpha + 1)}. \tag{34}$$

Fig. 4 is divided into four parts, showcasing the lower bound fuzzy findings for various fractional orders of  $\alpha$ . Figs. 4(a) and 4(c) present the lower bound surfaces results with space coordinates  $\mu = 0.4$ ,  $0 \leq \mathfrak{R} \leq 3$ ,  $0 \leq \mathfrak{S} \leq 3$  upon  $\alpha = 0.5$  and  $\alpha = 1$  respectively. Similarly, Figs. 4(b) and 4(d) reveal the lower bound contour results with space components  $\mu = 0.4$ ,  $-1 \leq \mathfrak{R} \leq 1$ ,  $-1 \leq \mathfrak{S} \leq 1$  upon  $\alpha = 0.5$  and  $\alpha = 1$  respectively. Fig. 5 is divided into four parts, showcasing the upper bound fuzzy findings for various fractional orders of  $\alpha$ . Figs. 5(a) and 5(c) present the upper bound surfaces results with space components  $\mu = 0.4$ ,  $0 \leq \mathfrak{R} \leq 1$ ,  $0 \leq \mathfrak{S} \leq 1$  upon  $\alpha = 0.5$  and  $\alpha = 1$  respectively. Similarly, Figs. 5(b) and 5(d) reveal the upper bound contour results with space components  $\mu = 0.4$ ,  $0 \leq \mathfrak{R} \leq 1$ ,  $0 \leq \mathfrak{S} \leq 1$  upon  $\alpha = 0.5$  and  $\alpha = 1$  respectively. We consider the amount of  $\vartheta = 0.1$  for lower and upper bound surface and contour fuzzy results respectively. On observing, the fractional order on both values gives excellent results to show that our proposed approach is legitimate and robust for the fuzzy fractional problems. Fig. 6 states the 2D fuzzy plot for lower and upper bound results when  $\mu = 0.4$  and  $\mu = 0.8$ .

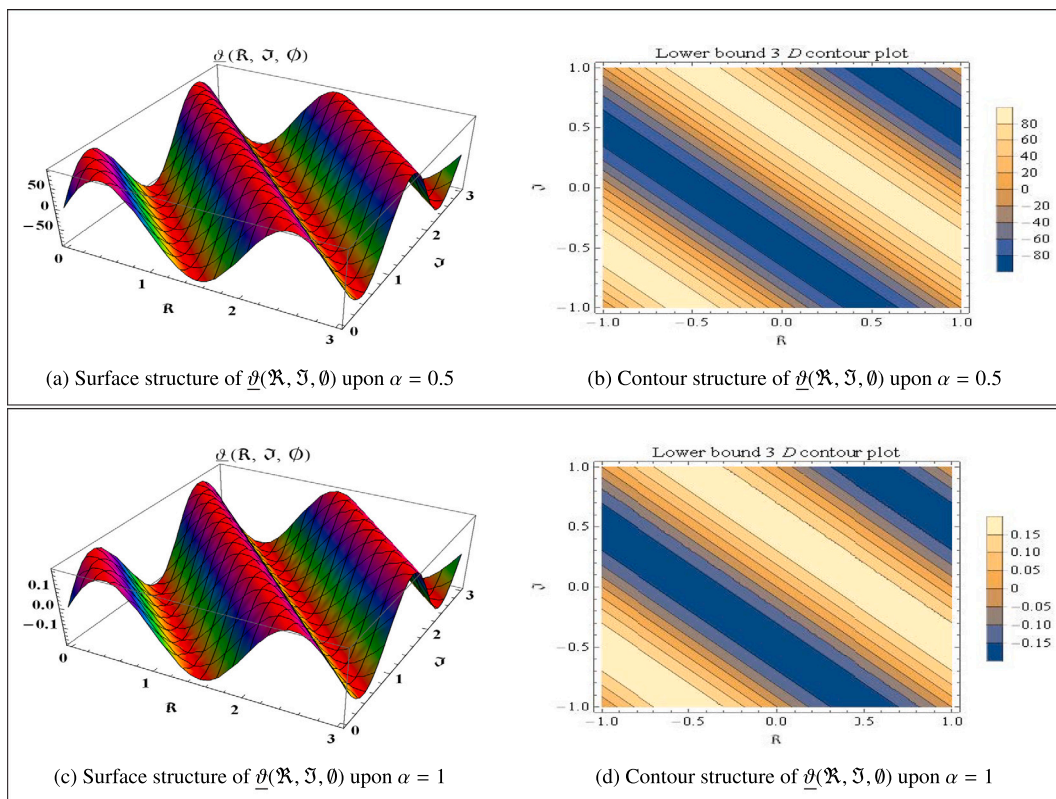


Fig. 4. 3D surface and contour plots of  $\underline{\theta}(\mathfrak{R}, \mathfrak{J}, \theta)$  solutions with  $\alpha = 0.5, 1$  for Example (4.2).

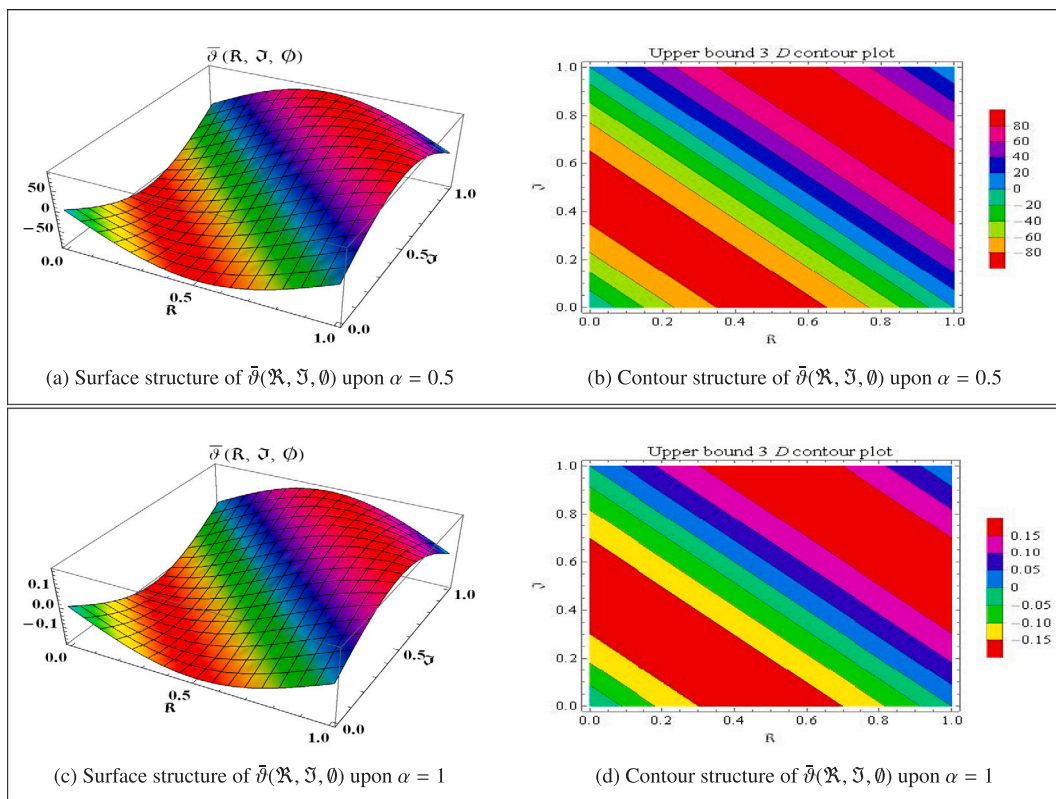


Fig. 5. 3D surface and contour plots of  $\bar{\theta}(\mathfrak{R}, \mathfrak{J}, \theta)$  solutions with  $\alpha = 0.5, 1$  for Example (4.2).

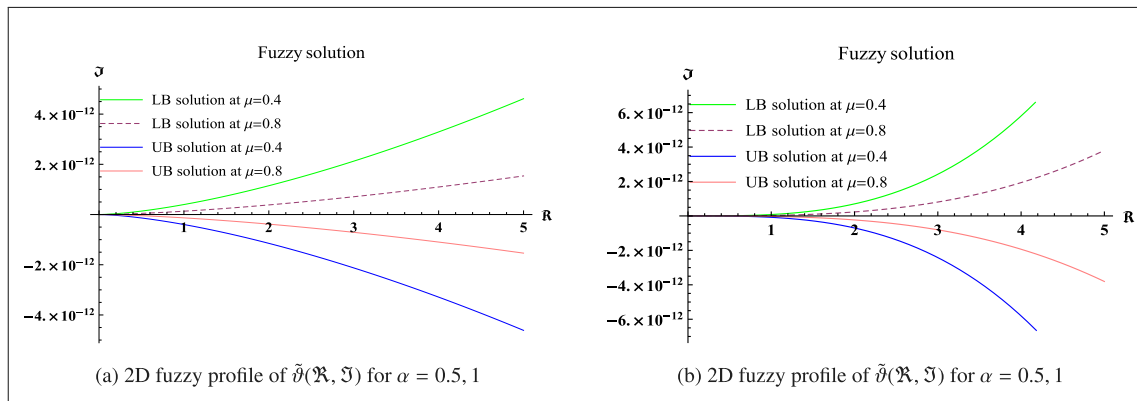


Fig. 6. 2D fuzzy  $\tilde{\theta}(\mathfrak{R}, \mathfrak{T})$  solutions on different fractional order for Example (4.2).

4.3. Example 3

Let us examine another two-dimensional time-fractional fuzzy heat problem

$$D_{\theta}^{\alpha} \tilde{\theta}(\mathfrak{R}, \mathfrak{T}, \theta) = \frac{1}{2}(\mathfrak{R} + \mathfrak{T})^2 \left[ \tilde{\theta}_{\mathfrak{R}\mathfrak{R}}(\mathfrak{R}, \mathfrak{T}, \theta) + \tilde{\theta}_{\mathfrak{T}\mathfrak{T}}(\mathfrak{R}, \mathfrak{T}, \theta) \right] + \mathfrak{R} + \mathfrak{T} + \theta^4, \quad (35)$$

with the initial condition

$$\tilde{\theta}(\mathfrak{R}, \mathfrak{T}, 0) = \tilde{\omega}(\mathfrak{R} + \mathfrak{T})^2. \quad (36)$$

here  $\tilde{\omega} = [\underline{\omega}, \bar{\omega}] = [\mu - 1, 1 - \mu]$ .

4.3.1. Lower bound findings for  $\tilde{\theta}(\mathfrak{R}, \mathfrak{T}, \theta)$

From Eq. (35), we can write the lower bound fuzzy problem as follows

$$\frac{\partial^{\alpha} \theta}{\partial \theta^{\alpha}} = \frac{1}{2}(\mathfrak{R} + \mathfrak{T})^2 \left( \frac{\partial^2 \theta}{\partial \mathfrak{R}^2} + \frac{\partial^2 \theta}{\partial \mathfrak{T}^2} \right) + \mathfrak{R} + \mathfrak{T} + \theta^4, \quad (37)$$

with the initial condition

$$\underline{\theta}(\mathfrak{R}, \mathfrak{T}, 0) = (\mu - 1)(\mathfrak{R} + \mathfrak{T})^2. \quad (38)$$

Using the aforementioned approach, we receive the subsequent outcomes:

$$\underline{\theta}_0(\mathfrak{R}, \mathfrak{T}, \theta) = (\mu - 1)(\mathfrak{R} + \mathfrak{T})^2 + \mathfrak{R} \frac{\theta^{\alpha}}{\Gamma(\alpha + 1)} + \mathfrak{T} \frac{\theta^{\alpha}}{\Gamma(\alpha + 1)} + 24 \frac{\theta^{\alpha+4}}{\Gamma(\alpha + 5)},$$

$$\underline{\theta}_1(\mathfrak{R}, \mathfrak{T}, \theta) = 2(\mu - 1)(\mathfrak{R} + \mathfrak{T})^2 \frac{\theta^{\alpha}}{\Gamma(\alpha + 1)},$$

$$\underline{\theta}_2(\mathfrak{R}, \mathfrak{T}, \theta) = 4(\mu - 1)(\mathfrak{R} + \mathfrak{T})^2 \frac{\theta^{2\alpha}}{\Gamma(2\alpha + 1)},$$

$$\underline{\theta}_3(\mathfrak{R}, \mathfrak{T}, \theta) = 8(\mu - 1)(\mathfrak{R} + \mathfrak{T})^2 \frac{\theta^{3\alpha}}{\Gamma(3\alpha + 1)},$$

⋮

Consequently, these results can be written as follows:

$$\begin{aligned} \underline{\theta}(\mathfrak{R}, \mathfrak{T}, \theta) &= (\mu - 1)(\mathfrak{R} + \mathfrak{T})^2 + \mathfrak{R} \frac{\theta^{\alpha}}{\Gamma(\alpha + 1)} + \mathfrak{T} \frac{\theta^{\alpha}}{\Gamma(\alpha + 1)} + 24 \frac{\theta^{\alpha+4}}{\Gamma(\alpha + 5)} \\ &+ 2(\mu - 1)(\mathfrak{R} + \mathfrak{T})^2 \frac{\theta^{\alpha}}{\Gamma(\alpha + 1)} \\ &+ 4(\mu - 1)(\mathfrak{R} + \mathfrak{T})^2 \frac{\theta^{2\alpha}}{\Gamma(2\alpha + 1)} \\ &+ 8(\mu - 1)(\mathfrak{R} + \mathfrak{T})^2 \frac{\theta^{3\alpha}}{\Gamma(3\alpha + 1)} + \dots \end{aligned} \quad (39)$$

**Remark.** If  $g(\mathfrak{R}, \mathfrak{T}, \theta) = 0$ , then above equation becomes as

$$\begin{aligned} \underline{\theta}(\mathfrak{R}, \mathfrak{T}, \theta) &= (\mu - 1)(\mathfrak{R} + \mathfrak{T})^2 + 2(\mu - 1)(\mathfrak{R} + \mathfrak{T})^2 \frac{\theta^{\alpha}}{\Gamma(\alpha + 1)} \\ &+ 4(\mu - 1)(\mathfrak{R} + \mathfrak{T})^2 \frac{\theta^{2\alpha}}{\Gamma(2\alpha + 1)} \\ &+ 8(\mu - 1)(\mathfrak{R} + \mathfrak{T})^2 \frac{\theta^{3\alpha}}{\Gamma(3\alpha + 1)} + \dots \end{aligned} \quad (40)$$

It can be in closed form

$$\underline{\theta}(\mathfrak{R}, \mathfrak{T}, \theta) = (\mu - 1)(\mathfrak{R} + \mathfrak{T})^2 \sum_{n=0}^{\infty} \frac{(2\theta^{\alpha})^n}{\Gamma(n\alpha + 1)}. \quad (41)$$

4.3.2. Upper bound findings for  $\tilde{\theta}(\mathfrak{R}, \mathfrak{T}, \theta)$

From Eq. (35), we can write the upper bound fuzzy problem as follows

$$\frac{\partial^{\alpha} \bar{\theta}}{\partial \theta^{\alpha}} = \frac{1}{2}(\mathfrak{R} + \mathfrak{T})^2 \left( \frac{\partial^2 \bar{\theta}}{\partial \mathfrak{R}^2} + \frac{\partial^2 \bar{\theta}}{\partial \mathfrak{T}^2} \right) + \mathfrak{R} + \mathfrak{T} + \theta^4, \quad (42)$$

with the initial condition

$$\bar{\theta}(\mathfrak{R}, \mathfrak{T}, 0) = (1 - \mu)(\mathfrak{R} + \mathfrak{T})^2. \quad (43)$$

Using the aforementioned approach, we receive the subsequent outcomes:

$$\bar{\theta}_0(\mathfrak{R}, \mathfrak{T}, \theta) = (1 - \mu)(\mathfrak{R} + \mathfrak{T})^2 + \mathfrak{R} \frac{\theta^{\alpha}}{\Gamma(\alpha + 1)} + \mathfrak{T} \frac{\theta^{\alpha}}{\Gamma(\alpha + 1)} + 24 \frac{\theta^{\alpha+4}}{\Gamma(\alpha + 5)},$$

$$\bar{\theta}_1(\mathfrak{R}, \mathfrak{T}, \theta) = 2(1 - \mu)(\mathfrak{R} + \mathfrak{T})^2 \frac{\theta^{\alpha}}{\Gamma(\alpha + 1)},$$

$$\bar{\theta}_2(\mathfrak{R}, \mathfrak{T}, \theta) = 4(1 - \mu)(\mathfrak{R} + \mathfrak{T})^2 \frac{\theta^{2\alpha}}{\Gamma(2\alpha + 1)},$$

$$\bar{\theta}_3(\mathfrak{R}, \mathfrak{T}, \theta) = 8(1 - \mu)(\mathfrak{R} + \mathfrak{T})^2 \frac{\theta^{3\alpha}}{\Gamma(3\alpha + 1)},$$

⋮

Consequently, these results can be written as follows:

$$\begin{aligned} \bar{\theta}(\mathfrak{R}, \mathfrak{T}, \theta) &= (1 - \mu)(\mathfrak{R} + \mathfrak{T})^2 + \mathfrak{R} \frac{\theta^{\alpha}}{\Gamma(\alpha + 1)} + \mathfrak{T} \frac{\theta^{\alpha}}{\Gamma(\alpha + 1)} + 24 \frac{\theta^{\alpha+4}}{\Gamma(\alpha + 5)} \\ &+ 2(1 - \mu)(\mathfrak{R} + \mathfrak{T})^2 \frac{\theta^{\alpha}}{\Gamma(\alpha + 1)} \\ &+ 4(1 - \mu)(\mathfrak{R} + \mathfrak{T})^2 \frac{\theta^{2\alpha}}{\Gamma(2\alpha + 1)} \\ &+ 8(1 - \mu)(\mathfrak{R} + \mathfrak{T})^2 \frac{\theta^{3\alpha}}{\Gamma(3\alpha + 1)} + \dots \end{aligned} \quad (44)$$

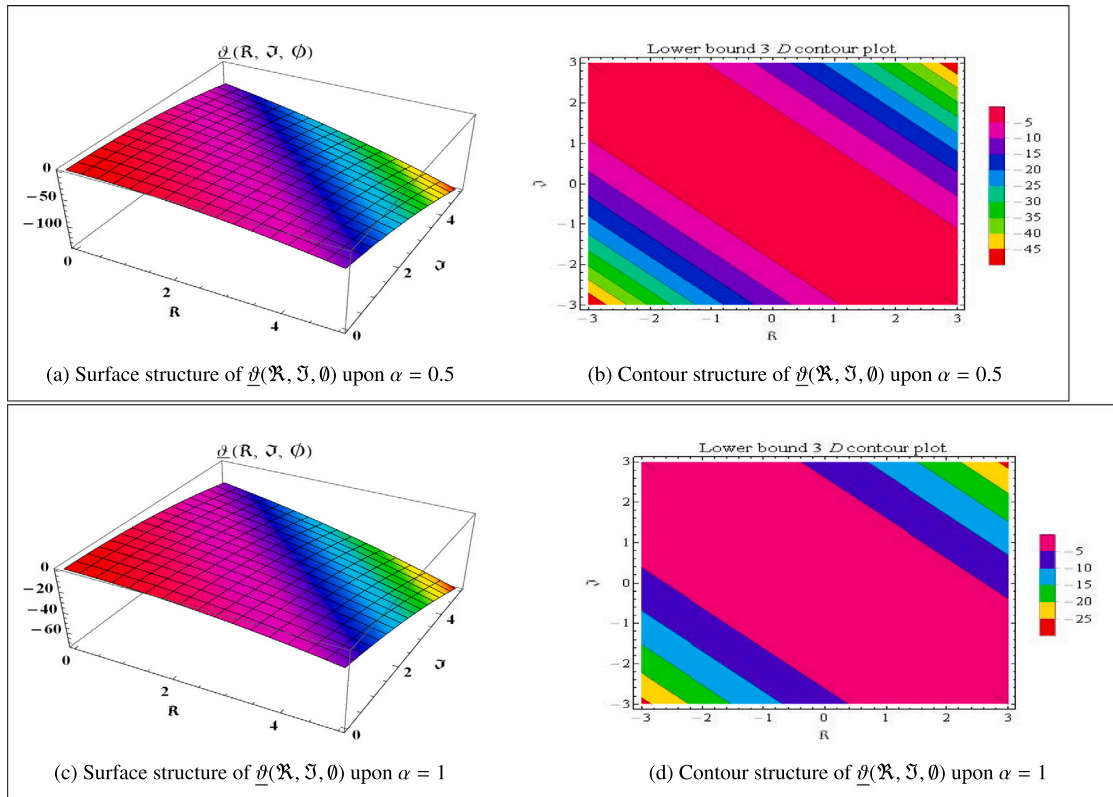


Fig. 7. 3D surface and contour plots of  $\underline{\vartheta}(\mathfrak{R}, \mathfrak{I}, \phi)$  solutions with  $\alpha = 0.5, 1$  for Example (4.3).

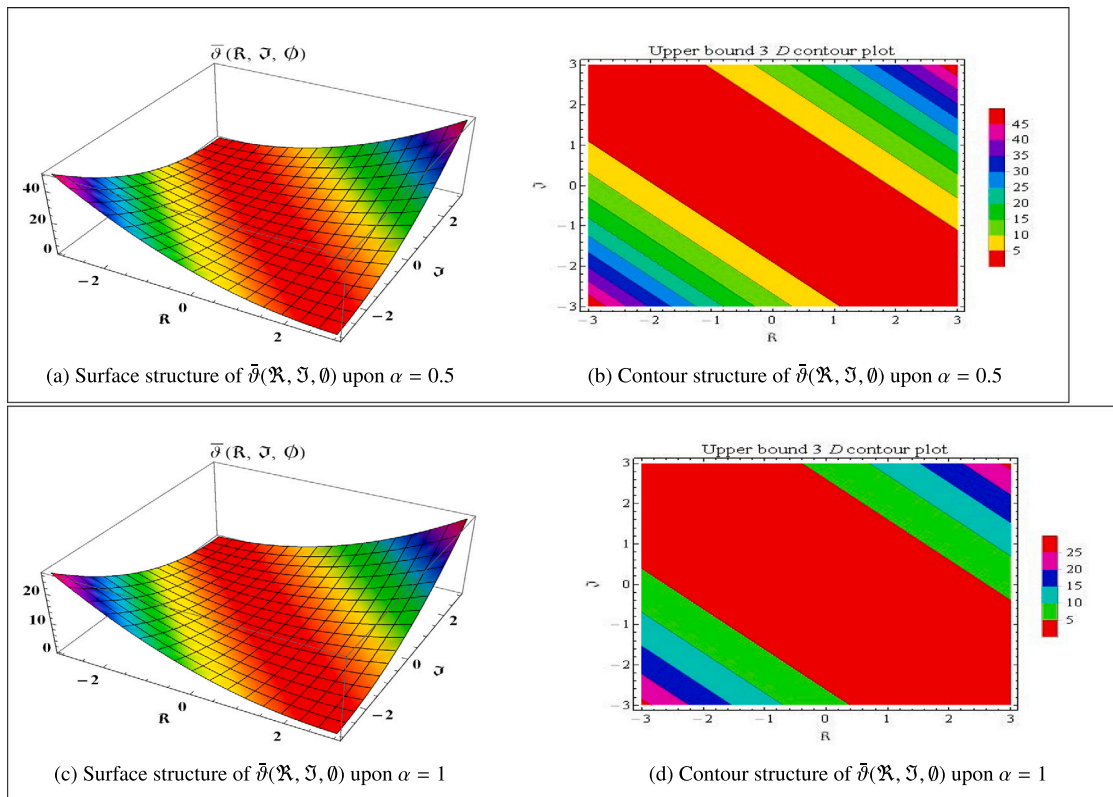


Fig. 8. 3D surface and contour plots of  $\overline{\vartheta}(\mathfrak{R}, \mathfrak{I}, \phi)$  solutions with  $\alpha = 0.5, 1$  for Example (4.3).

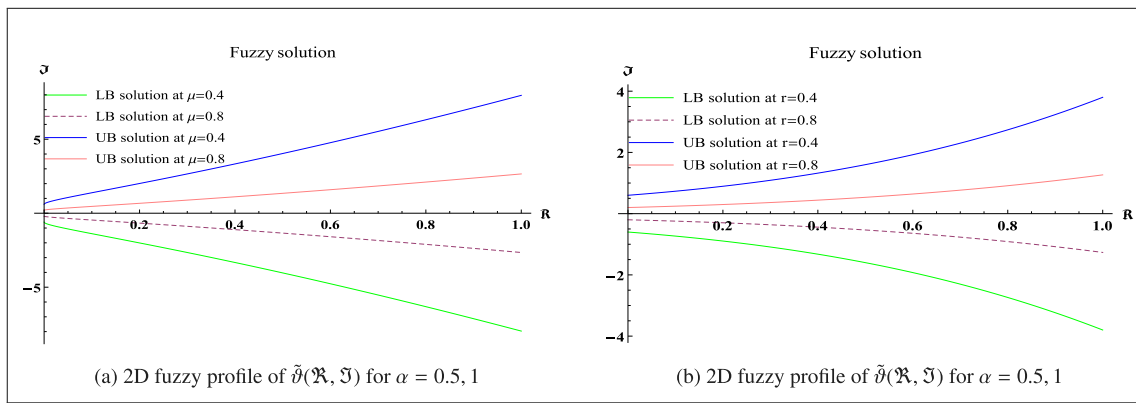


Fig. 9. 2D fuzzy  $\tilde{\theta}(\mathfrak{R}, \mathfrak{S})$  solutions on different fractional order for Example (4.3).

**Remark.** If  $g(\mathfrak{R}, \mathfrak{S}, \theta) = 0$ , then above equation becomes as

$$\begin{aligned} \tilde{\theta}(\mathfrak{R}, \mathfrak{S}, \theta) &= (1 - \mu)(\mathfrak{R} + \mathfrak{S})^2 + 2(1 - \mu)(\mathfrak{R} + \mathfrak{S})^2 \frac{\theta^\alpha}{\Gamma(\alpha + 1)} \\ &+ 4(1 - \mu)(\mathfrak{R} + \mathfrak{S})^2 \frac{\theta^{2\alpha}}{\Gamma(2\alpha + 1)} \\ &+ 8(1 - \mu)(\mathfrak{R} + \mathfrak{S})^2 \frac{\theta^{3\alpha}}{\Gamma(3\alpha + 1)} + \dots \end{aligned} \quad (45)$$

It can be in closed form

$$\tilde{\theta}(\mathfrak{R}, \mathfrak{S}, \theta) = (1 - \mu)(\mathfrak{R} + \mathfrak{S})^2 \sum_{n=0}^{\infty} \frac{(2\theta^\alpha)^n}{\Gamma(n\alpha + 1)}. \quad (46)$$

Fig. 7 is divided into four parts, showcasing the lower bound fuzzy findings for various fractional orders of  $\alpha$ . Figs. 7(a) and 7(c) present the lower bound surfaces results with space coordinates  $\mu = 0.4$ ,  $0 \leq \mathfrak{R} \leq 5$ ,  $0 \leq \mathfrak{S} \leq 5$  upon  $\alpha = 0.5$  and  $\alpha = 1$  respectively. Similarly, Figs. 7(b) and 7(d) reveal the lower bound contour results with space components  $\mu = 0.4$ ,  $-3 \leq \mathfrak{R} \leq 3$ ,  $-3 \leq \mathfrak{S} \leq 3$  upon  $\alpha = 0.5$  and  $\alpha = 1$  respectively. Fig. 8 is divided into four parts, showcasing the upper bound fuzzy findings for various fractional orders of  $\alpha$ . Figs. 8(a) and 8(c) present the upper surfaces results with space components  $\mu = 0.4$ ,  $-3 \leq \mathfrak{R} \leq 3$ ,  $-3 \leq \mathfrak{S} \leq 3$  upon  $\alpha = 0.5$  and  $\alpha = 1$  respectively. Similarly, Figs. 8(b) and 8(d) reveal the upper bound contour results with space components  $\mu = 0.4$ ,  $-3 \leq \mathfrak{R} \leq 3$ ,  $-3 \leq \mathfrak{S} \leq 3$  upon  $\alpha = 0.5$  and  $\alpha = 1$  respectively. We consider the amount of  $\theta = 0.1$  for lower and upper bound surface and contour fuzzy results respectively. On observing, the fractional order on both values gives excellent results to show that our proposed approach is legitimate and robust for the fuzzy fractional problems. Fig. 9 states the 2D fuzzy plot for lower and upper bound results when  $\mu = 0.4$  and  $\mu = 0.8$ .

### 5. Conclusion

In this work, we have successfully derived the outcomes of a 2D heat problem with fuzzy fractional order in the presence of some source terms. We examine the fractional derivatives in the Caputo sense. The primary benefit of utilizing the Caputo derivative is its capacity to present the system more precisely with memory effects and long-range interactions when compared to conventional integer-order derivatives. Our proposed approach is more efficient and time-saving compared to the classical RPSS. The ST is capable of linear problems only, so we introduce RPSS to handle the nonlinear terms where the results can be obtained in the form of a series solution. We have plotted various graphs in different fractional order and captured the significance results. The lower and upper-bound solutions are illustrated through contour and surface depictions at various parameters of fractional order  $\alpha$ . The accuracy and capability of the suggested approach are demonstrated through the use of surface and contour plots. The physical model that exhibits characteristics such as uncertainty, non-linearity,

and ambiguity in the fractional problems of science and engineering may be handled using fuzzy logic, and as a result, our approach can be conveniently utilized for these models in the future.

### CRedit authorship contribution statement

**Jinxing Liu:** Writing – original draft, Methodology. **Muhammad Nadeem:** Supervision, Investigation. **Ali Hasan Ali:** Project administration, Funding acquisition. **Fawziah M. Alotaibi:** Visualization, Validation. **Loredana Florentina Iambor:** Formal analysis, Data curation.

### Declaration of competing interest

The authors declare that they have no known competing financial interests or personal relationships that could have appeared to influence the work reported in this paper.

### Acknowledgments

The authors would like to acknowledge Deanship of Graduate Studies and Scientific Research, Taif University, Saudi Arabia for funding this work.

### References

- [1] D. Baleanu, Y. Karaca, L. Vázquez, J.E. Macías-Díaz, Advanced fractional calculus, differential equations and neural networks: Analysis, modeling and numerical computations, *Phys. Scr.* 98 (11) (2023) 110201.
- [2] Y. Xu, Y. Li, D. Liu, A method to stochastic dynamical systems with strong nonlinearity and fractional damping, *Nonlinear Dynam.* 83 (2016) 2311–2321.
- [3] I. Podlubny, Geometric and physical interpretation of fractional integration and fractional differentiation, *Fract. Calc. Appl. Anal.* 5 (4) (2001) 367–386.
- [4] O. Tasbozan, Y. Çenesiz, A. Kurt, D. Baleanu, New analytical solutions for conformable fractional PDEs arising in mathematical physics by exp-function method, *Open Phys.* 15 (1) (2017) 647–651.
- [5] S. Kumar, V. Gupta, An application of variational iteration method for solving fuzzy time-fractional diffusion equations, *Neural Comput. Appl.* 33 (2021) 17659–17668.
- [6] N. Van Hoa, Fuzzy fractional functional differential equations under Caputo gh-differentiability, *Commun. Nonlinear Sci. Numer. Simul.* 22 (1–3) (2015) 1134–1157.
- [7] O. Abu Arqub, J. Singh, B. Maayah, M. Alhodaly, Reproducing kernel approach for numerical solutions of fuzzy fractional initial value problems under the Mittag-Leffler kernel differential operator, *Math. Methods Appl. Sci.* 46 (7) (2023) 7965–7986.
- [8] H. Zhang, X. Liao, J. Yu, Fuzzy modeling and synchronization of hyperchaotic systems, *Chaos Solitons Fractals* 26 (3) (2005) 835–843.
- [9] A. Farajzadeh, A. Hosseinpour, W. Kumam, On boundary value problems in normed fuzzy spaces, *Thai J. Math.* 20 (1) (2022) 305–313.
- [10] A. Ali, I. Suwan, T. Abdeljawad, et al., Numerical simulation of time partial fractional diffusion model by Laplace transform, *AIMS Math.* 7 (2) (2022) 2878–2890.

- [11] M. Arfan, K. Shah, A. Ullah, S. Salahshour, A. Ahmadian, M. Ferrara, A novel semi-analytical method for solutions of two dimensional fuzzy fractional wave equation using natural transform, *Discrete Contin. Dyn. Syst.-S* 15 (2) (2022) 315–338.
- [12] M. Osman, A. Almahi, O.A. Omer, A.M. Mustafa, S.A. Altaie, Approximation solution for fuzzy fractional-order partial differential equations, *Fractal Fract.* 6 (11) (2022) 646.
- [13] A.A. Hamoud, K. Ghadle, Homotopy analysis method for the first order fuzzy Volterra-Fredholm integro-differential equations, *Indonesian J. Electr. Eng. Comput. Sci.* 11 (3) (2018) 857–867.
- [14] M.R. Ali, A.R. Hadhoud, Application of haar wavelet method for solving the nonlinear fuzzy integro-differential equations, *J. Comput. Theor. Nanosci.* 16 (2) (2019) 365–372.
- [15] B. Maayah, O.A. Arqub, Uncertain M-fractional differential problems: existence, uniqueness, and approximations using Hilbert reproducing technique provisioner with the case application: series resistor-inductor circuit, *Phys. Scr.* 99 (2) (2024) 025220.
- [16] O. Abu Arqub, R. Mezghiche, B. Maayah, Fuzzy M-fractional integrodifferential models: theoretical existence and uniqueness results, and approximate solutions utilizing the Hilbert reproducing kernel algorithm, *Front. Phys.* 11 (2023) 1252919.
- [17] O.A. Arqub, M. Al-Smadi, Fuzzy conformable fractional differential equations: novel extended approach and new numerical solutions, *Soft Comput.* 24 (16) (2020) 12501–12522.
- [18] M. Arfan, K. Shah, T. Abdeljawad, Z. Hammouch, An efficient tool for solving two-dimensional fuzzy fractional-ordered heat equation, *Numer. Methods Partial Differential Equations* 37 (2) (2021) 1407–1418.
- [19] S. Narayanamoorthy, S. Sathiyapriya, A pertinent approach to solve nonlinear fuzzy integro-differential equations, *SpringerPlus* 5 (1) (2016) 1–17.
- [20] V.P. Dubey, R. Kumar, D. Kumar, A reliable treatment of residual power series method for time-fractional Black–Scholes European option pricing equations, *Phys. A* 533 (2019) 122040.
- [21] V.A. Vijesh, A short note on the quasilinearization method for fractional differential equations, *Numer. Funct. Anal. Optim.* 37 (9) (2016) 1158–1167.
- [22] N.T. Shawagfeh, Analytical approximate solutions for nonlinear fractional differential equations, *Appl. Math. Comput.* 131 (2–3) (2002) 517–529.
- [23] A. Prakash, H. Kaur, A new numerical method for a fractional model of non-linear Zakharov–Kuznetsov equations via Sumudu transform, 2019, pp. 189–204.
- [24] M. Goyal, A. Prakash, S. Gupta, An efficient perturbation sumudu transform technique for the time-fractional vibration equation with a memory dependent fractional derivative in Liouville–Caputo sense, *Int. J. Appl. Comput. Math.* 7 (2021) 1–18.
- [25] M.A. Bayrak, A. Demir, A new approach for space-time fractional partial differential equations by residual power series method, *Appl. Math. Comput.* 336 (2018) 215–230.
- [26] O.A. Arqub, Series solution of fuzzy differential equations under strongly generalized differentiability, *J. Adv. Res. Appl. Math.* 5 (1) (2013) 31–52.
- [27] O.A. Arqub, A. El-Ajou, Z.A. Zhou, S. Momani, Multiple solutions of nonlinear boundary value problems of fractional order: a new analytic iterative technique, *Entropy* 16 (1) (2014) 471–493.
- [28] M. Alquran, Analytical solutions of fractional foam drainage equation by residual power series method, *Math. Sci.* 8 (4) (2014) 153–160.
- [29] G. Arora, R. Pant, H. Emadifar, M. Khademi, Numerical solution of fractional relaxation–oscillation equation by using residual power series method, *Alex. Eng. J.* 73 (2023) 249–257.
- [30] Z. Korpınar, M. Inc, E. Hınçal, D. Baleanu, Residual power series algorithm for fractional cancer tumor models, *Alex. Eng. J.* 59 (3) (2020) 1405–1412.
- [31] S. Hasan, A. Al-Zoubi, A. Freihet, M. Al-Smadi, S. Momani, Solution of fractional SIR epidemic model using residual power series method, *Appl. Math. Inf. Sci.* 13 (2) (2019) 153–161.
- [32] G.M. Ismail, H.R. Abdl-Rahim, H. Ahmad, Y.-M. Chu, Fractional residual power series method for the analytical and approximate studies of fractional physical phenomena, *Open Phys.* 18 (1) (2020) 799–805.